CORA Cork Open Research Archive
Cartlann Taighde Oscailte Chorcaí

Title	Dual wave farms for energy production and coastal protection under sea level rise
Authors	Rodriguez-Delgado, Cristobal;Bergillos, Rafael J.;Iglesias, Gregorio
Publication date	2019-03-09
Original Citation	Rodriguez-Delgado, C., Bergillos, R. J. and Iglesias, G. (2019) 'Dual wave farms for energy production and coastal protection under sea level rise', Journal of Cleaner Production, 222, pp. 364-372. doi: 10.1016/j.jclepro.2019.03.058
Type of publication	Article (peer-reviewed)
Link to publisher's version	http://www.sciencedirect.com/science/article/pii/S0959652619307474 - 10.1016/j.jclepro.2019.03.058
Rights	© 2019, Elsevier Ltd. All rights reserved. This manuscript version is made available under the CC BY-NC-ND 4.0 license. - https://creativecommons.org/licenses/by-nc-nd/4.0/
Download date	2026-11-01 02:11:28
Item downloaded from	https://hdl.handle.net/10468/7740



UCC
University College Cork, Ireland
Coláiste na hOllscoile Corcaigh

Dual wave farms for energy production and coastal protection under sea level rise

Cristobal Rodriguez-Delgado[a,b], Rafael J. Bergillos[c,*], Gregorio Iglesias[d,a]

[a] *School of Engineering, University of Plymouth, Plymouth PL4 8AA, UK*
[b] *PROES Consultores, Calle San Germán 39, 28020 Madrid, Spain*
[c] *Hydraulic Engineering Area, Department of Agronomy, University of Córdoba, Campus Rabanales, Leonardo Da Vinci Building, 14071 Córdoba, Spain*
[d] *MaREI, Environmental Research Institute & School of Engineering, University College Cork, College Road, Cork, Ireland*

Abstract

Climate change is poised to exacerbate coastal erosion. Recent research has presented a novel strategy to tackle this issue: dual wave farms, i.e., arrays of wave energy converters with the dual function of carbon-free energy generation and coastal erosion mitigation. However, the implications of sea level rise – another consequence of climate change – for the effectiveness of wave farms as coastal defence elements against shoreline erosion have not been studied so far. The objective of this work is to investigate how the coastal defence performance of a dual wave farm is affected by sea level rise through a case study (Playa Granada, southern Iberian Peninsula). To this end, a spectral wave propagation model, a longshore sediment transport formulation and a one-line model are combined to obtain the final subaerial beach areas for three sea level rise scenarios: the present situation, an optimistic and a pessimistic projection. These scenarios were modelled with and without the wave farm to assess its effects. We find that the dual wave farm reduces erosion and promotes accretion regardless of the sea level rise scenario considered. In the case of westerly storms, the dual wave farm is particularly effective: erosion is transformed into accretion. In general, and importantly, sea level rise strengthens the effectiveness of the dual wave farm

*Corresponding author.
E-mail address: rafael.bergillos@uco.es (R.J. Bergillos)

as a coastal protection mechanism. This fact enhances the competitiveness of wave farms as coastal defence elements.
Keywords: Renewable energy; Wave energy; climate change; sea level rise; coastal protection; sustainable development

1. Introduction

The large-scale exploitation of fossil fuels that started with the Industrial Revolution has caused serious environmental repercussions [1–4], including sea level rise and climate change [5, 6]. One of the most important challenges in the 21st century is to mitigate these repercussions in as much as possible, not least by developing new kinds of sustainable, carbon-free energies [7–19]. In this sense, ocean energies, and wave energy in particular, stand out as one of the most important due to the high resource availability [20–22].

Previous research in wave energy has focused on different aspects related to its exploitation: (i) the development of new technologies [23–29], (ii) the availability of the resource [30–37], (iii) synergies with other types of offshore renewable energies [38–40] and (iv) economic aspects [41–44]. However, the relation between this kind of technology and the incoming sea level rise still needs further research work if wave energy is going to be poised as a functional carbon-free energy in the near future.

Future sea level rise is becoming a threat for coasts across the world, increasing hazards like coastal flooding [45–47]. Among them, coasts near river deltas are being primarily affected, since they allocate places with high economic, social and environmental importance. In addition, anthropogenic interventions on their catchment areas are increasing other hazards as coastal erosion [48, 49].

One of the advantages of wave farms, i.e. arrays of wave energy converters (WECs), is the reduction in wave power in their lee. When waves are transmitted through the farm, part of their energy is absorbed. On these grounds, wave farms can be used to mitigate coastal erosion [50–55] and flooding [56]. In fact, dual wave farms have been defined as those designed to fulfil both functions:

carbon-free energy generation and coastal defence [57, 58]. Nevertheless, the wave farm effects on longshore sediment transport (LST), shoreline evolution and dry beach area availability under sea level rise have not been analyzed fo far. This analysis is necessary and relevant since sea level rise is one of the most dangerous consequences of climate change and induces changes on wave propagation and sediment transport patterns.

The objective of this work is to investigate the effects of sea level rise on the functionality of a wave farm for coastal protection against shoreline erosion. To this end, three sea level scenarios were analysed: the present situation (baseline), and the water level in 2100 according to optimistic (RCP4.5) and pessimistic (RCP8.5) projections proposed by [5]. A third-generation wave propagation model (SWAN) was applied to two case studies, with and without a wave farm, on a gravel dominated beach: Playa Granada (Southern Iberian Peninsula). The evolution of the shoreline was computed using a LST formulation [59] and a one-line model [60] in order to obtain the variations in subaerial beach area. The following sections describe the study area (Section 2), methodology (Section 3), results (Section 4), discussion (Section 5 and conclusions (Section 6) of this work.

2. Study area

Playa Granada is a 3-km-long beach located on the southern coast of Spain that faces the Mediterranean Sea (Figure 1). The beach corresponds to the central stretch of the Guadalfeo deltaic coast and is bounded to the west by the Guadalfeo River mouth and to the east by *Punta del Santo*, the former location of the river mouth [61, 62]. The deltaic coast is bounded to the west by Salobreña Rock and to the east by Motril Port.

The state of the beach profile is practically reflective and the morphodynamic response of the beach is dominated by the gravel fraction [63, 64]. The studied stretch of beach has been experiencing shoreline retreat and terminal erosion in recent years (Fig. 1c), partly due to anthropogenic interventions in the

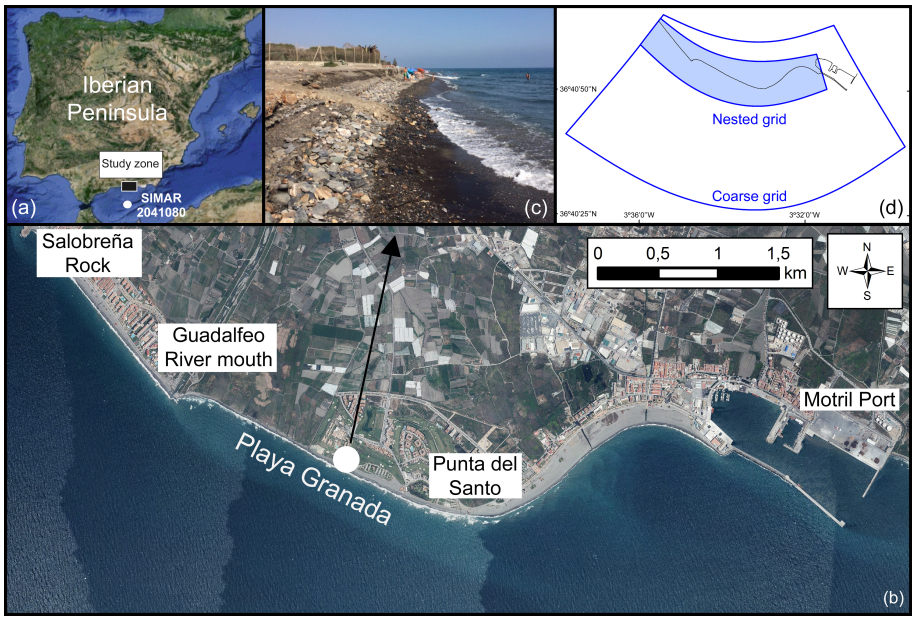


Figure 1: (a) Location of the study site in the southern part of the Iberian Peninsula. (b) Aerial photograph of the study site, including the locations of the main geographical features and structures. (c) Storm erosion in Playa Granada. (d) Computational domains used in the numerical model.

Guadalfeo River basin [61, 65]. As a result, artificial nourishment projects have been frequently performed over the past decade [66], but the long-term efficiency of these projects has been very limited [67, 68].

The region is subjected to the passage of extra-tropical Atlantic cyclones and Mediterranean storms [69]. The storm wave climate is distinctly bimodal with the prevailing west-southwest (extra-tropical cyclones) and east-southeast (Mediterranean storms) wave directions [70]. Peak significant wave heights during typical and extreme storm events exceed 2.1 m and 3.1 m, respectively [71]. The astronomical tidal range is ~ 0.6 m (micro-tidal conditions), whereas typical storm surge levels can exceed 0.5 m [63].

3. Materials and methods

3.1. Modelled wave farm

The influence of wave energy extraction on the wave propagation and sediment transport of Playa Granada was studied modelling a wave farm off the coast, near Punta del Santo (Fig. 2). This wave farm was composed by eleven WECs, arranged in two rows. The location and layout of the wave farm were chosen based on the optimization for coastal defence purposes carried out in previous works [53, 54].

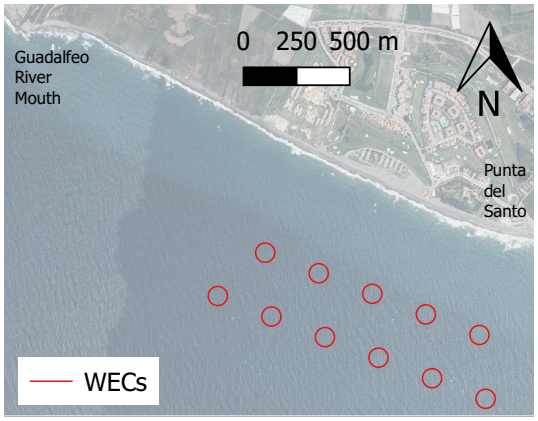


Figure 2: Wave farm location in front of Playa Granada.

The wave energy converter (WEC) selected for the analysis was WaveCat [72, 73]. This device, shown in Figure 3, is a floating and overtopping WEC that comprises two hulls joined by a hinge at the stern [73–75]. For a detailed description of the device, the reader is referred to [25, 76]. Wave farms consisting of WaveCat WECs have been proven to fulfil the dual function of wave energy generators and coastal defence (e.g., Rodriguez-Delgado et al. [57], Abanades et al. [58], among others). This device was included in the wave propagation numerical model through its transmission and reflection coefficients [25]. The inter-device spacing was set to $2D$, with $D = 90$ m the diameter of WaveCat. In order to properly investigate the effects of the wave farm, the baseline (no wave farm) situation was also analysed.

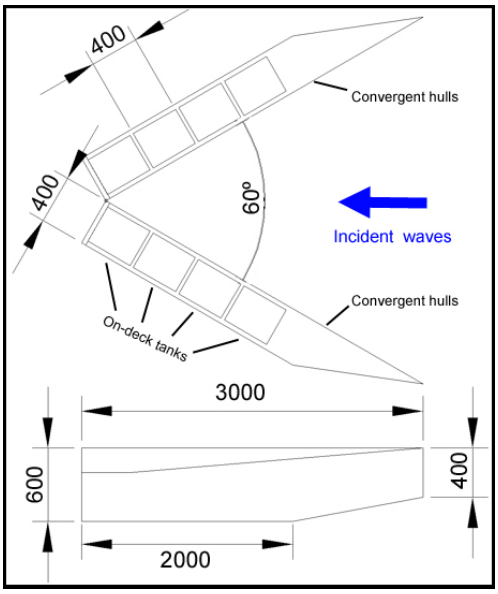


Figure 3: Geometry of the WaveCat device at a 1:30 scale (dimensions in mm).

3.2. Wave and water level conditions

The response of the shoreline was modelled at the storm time scale; more specifically, two sea states were studied, corresponding to westerly and easterly storms – the two prevailing wave directions at the study site. The most frequent values of significant wave height and peak period for storm conditions were selected (Table 1).

Table 1: Parameters of the sea states. [H_s: significant wave height, T_p: peak period, θ: mean wave direction].

	H_s (m)	T_p (s)	θ (°)
West	3.1	8.4	238
East	3.1	8.4	107

These sea states were applied to three scenarios: the present situation (SLR0), and the optimistic (SLR1) and pessimistic projections (SLR2) of sea level rise in 2100, according to the representative concentration pathways (RCP) 4.5 and 8.5 proposed by [5] for the study site.

3.3. Wave propagation model

The influence of wave farm and sea level rise in the wave field was computed by means of the third-generation wave propagation model SWAN [77]. This numerical model is able to simulate the effects of obstacles on wave propagation patterns, i.e., reduction of the wave height propagating behind or over the obstacle along its length, reflection of the waves that impinge the obstacle, and diffraction of the waves around its boundaries [37, 78, 79].

The WaveCat WECs were thus included as obstacles in the numerical model, using transmission and reflection coefficients obtained in laboratory experiments [25]. Two computational grids were used (Fig. 1): (i) a coarse grid, covering the region from deep water to the nearshore, with cell sizes that decrease with depth from 170x65 m to 80x80 m; and (ii) a nested grid, covering the inshore region and wave farm area, with cell sizes of approximately 25x15 m. The cell size of the nested grid was adjusted to reproduce properly the effects of each WEC.

The spectral resolution of the frequency space consisted of 37 logarithmically distributed frequencies ranging from 0.03 to 1 Hz. For the directional space, the 360° were covered by 72 directions in increments of 5°. This model was previously calibrated and validated in the study area using data from extensive field campaigns [67]. SWAN results were used to obtain wave parameters at breaking, which are the basis of the LST formulation.

3.4. LST formulation and one-line model

LST rates in the study site for each sea level rise scenario, with and without wave farm, were computed using the formulation of [59] (Eq. 1). This equation has been proved to provide accurate results in a wide range of beach types, from sandy to gravel beaches. More to the point, it has been applied in the study site and successfully validated against field data [67]. The formula can be expressed as follows:

$$Q = 0.00018 K_{swell} \rho_s g^{0.5} \left(\tan\beta\right)^{0.4} \left(d_{50}\right)^{-0.6} \left(H_{s,br}\right)^{3.1} \sin\left(2\theta_{br}\right), \qquad (1)$$

where Q stands for the LST rate, $\rho_s = 2650$ kg/m^3 is the sediment density, $g = 9.81$ m/s^2 the acceleration of gravity, $d_{50} = 0.02$ m the sediment size, $\tan\beta$ the slope of the surf zone, $H_{s,br}$ the significant wave height at the breaking line, θ_{br} the mean wave direction at breaking and K_{swell} is a parameter which takes into account the effect of the wave period and varies between 1 and 1.5. This formulation was applied to compute LST rates for 341 beach profiles, evenly distributed, covering the stretch of coast between Salobreña Rock and Motril Port (Fig. 1).

The LST rates obtained were used to track changes in the shoreline position of each beach profile using the one-line model [60]. As in the case of the LST formulation, this model has been applied successfully to the study site in previous works [67]. The model equation is:

$$\frac{\partial y_s}{\partial t} = \frac{1}{D}\left(\frac{-\partial Q}{\partial x_s}\right), \tag{2}$$

with y_s and x_s the position of the shoreline, t the time, and D a representative length, taken as the summation of the berm height and the depth of closure.

4. Results

4.1. Wave farm interaction with the wave field

The changes in significant wave height at breaking, $H_{s,br}$, caused by the wave farm in the three sea level rise scenarios, are investigated in this section. More specifically, the ratio of the value of $H_{s,br}$ with the farm to that without the farm (baseline), hereafter referred to as the wave height ratio. The wave farm reduces the significant wave height at breaking in all cases (Fig. 4). This reduction is more significant in the case of the easterly storm than for the westerly storm: alongshore-averaged ratios range between 0.79 and 0.8 in the three sea level rise scenarios for the easterly storm (Fig. 4b), far smaller than those for the westerly storm, 0.97 - 0.98 (Fig. 4a).

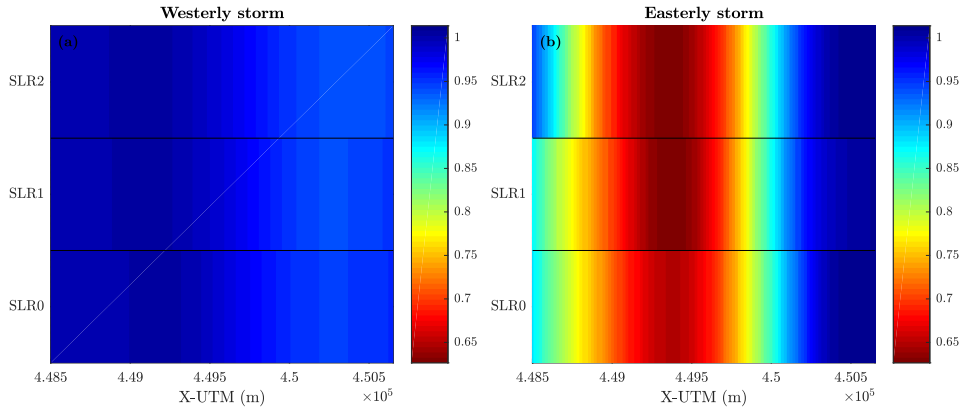


Figure 4: Ratio between the significant wave heights at breaking ($H_{s,br}$) with and without wave farm for the W (a) and E (b) storms.

When sea level rise is considered, the performance of the wave farm as coastal defence element improves slightly. In scenario SLR2, which has the largest sea level rise, the minimum wave height ratio for the westerly storm is 0.93. The corresponding values in scenarios SLR1 and SLR0 (baseline) are 0.94 and 0.95. In addition, with the increase in sea level, the shadow of the wave farm, i.e., the area of wave power deficit and consequently lower wave height, encompasses a greater length of coastline than in the baseline situation (Fig. 4). For the easterly storm, the differences between the optimistic and pessimistic projections for scenarios SLR1 and SLR2 are even smaller, with minimum wave height ratios of 0.63 in both cases. The minimum ratio rises up to 0.65 in SLR0.

4.2. LST rate variations

LST rates computed using the formulation of [59] are presented in this section. Sediment transport patterns are modified by the wave farm (Fig. 5). Under the westerly storm, these rates are reduced mainly in the eastern part of the study section, whereas the wave farm increases LST rates in the central part (Fig. 5a). Under the easterly storm, LST rates are reduced mainly in the central and western parts of Playa Granada, whereas the impact on the eastern end of the beach is lower (Fig. 5b). The differences between scenarios in the

eastern part of the beach under easterly storms are influenced by the effects of the shoreline horn (Punta del Santo, Fig. 2) on the propagation of easterly waves.

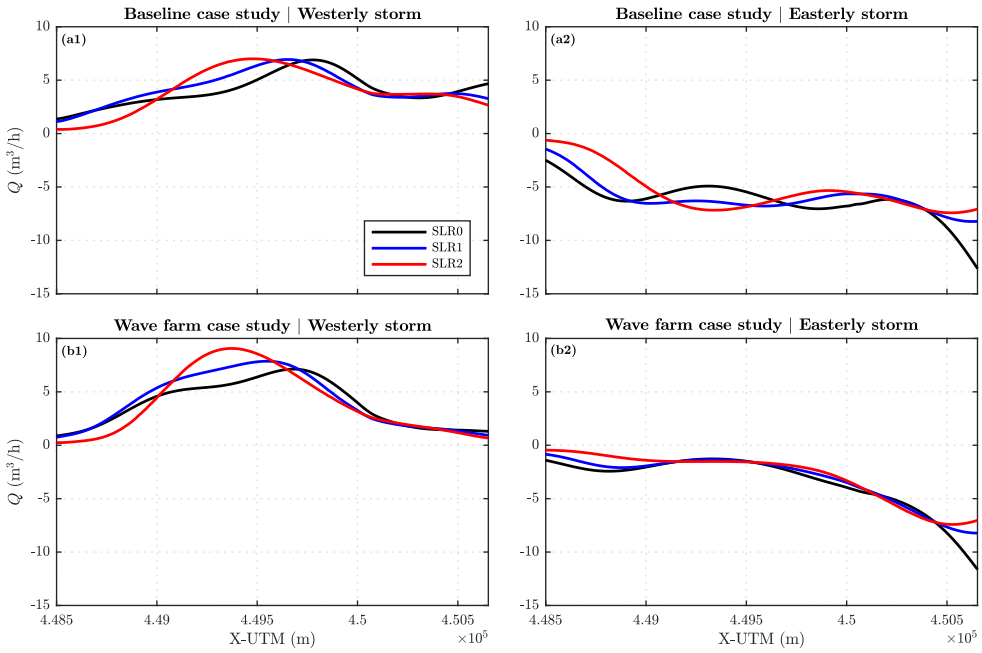


Figure 5: LST rate alongshore distribution without (a) and with (b) wave farm for the W (1) and E (2) storms.

This influence of the wave farm on LST patterns is readily analysed through the LST ratio, defined as the ratio between the LST rate with and without the wave farm (Figure 6). As described in the previous paragraph, under the westerly storm LST rates are increased in the central part, where maximum LST ratios of 1.53, 1.46, 1.45 are attained in scenarios SLR0, SLR1 and SLR2, respectively. On the contrary, in the western part of the beach the wave farm reduces LST rates, with minimum LST ratios as low as 0.28, 0.29 and 0.26, respectively (Fig. 6a). Sea level rise affects LST much as it does breaking wave heights, slightly increasing the positive impact of the wave farm; indeed, the alongshore-averaged LST ratio is higher in scenario SLR0 (0.95) than in scenarios SLR1 (0.93) and SLR2 (0.92).

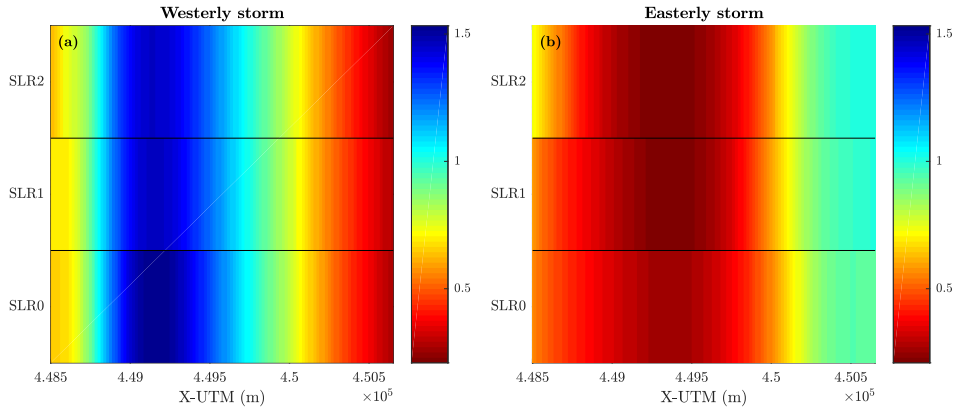


Figure 6: Ratio between the LST rates (Q) with and without wave farm for the W (a) and E (b) storms.

The modelled wave farm has a more intense impact under easterly storms. The minimum ratios, which are found in the central and western parts of the stretch of coast, are 0.26, 0.21 and 0.21 in SLR0, SLR1, SLR2, respectively (Fig. 6b). Conversely, in the eastern part of the beach, the impact is lower (ratios close to unity in the three sea level rise scenarios). This greater impact under the easterly storm is confirmed by the alongshore averaged ratios: 0.51, 0.50 and 0.52 for SLR0, SLR1 and SLR2, respectively.

4.3. Shoreline changes

LST rates computed in the previous section were the basis to apply the one-line model and assess changes in the shoreline caused by the sea states considered. The storms were modelled with a duration of 48 hours. The westerly storm causes erosion in the western part of the coast, whereas accretion appears in the eastern part (Fig. 7a1). Sea level rise modifies this behaviour, increasing erosion in the western part and reducing the advance of the shoreline in the central stretch. Maximum accretion is decreased; however, the shoreline advance is higher in the east end.

The easterly storm produces accretion in both ends of Playa Granada, with erosion appearing in the central stretch (Fig. 7a2). In this case, sea level

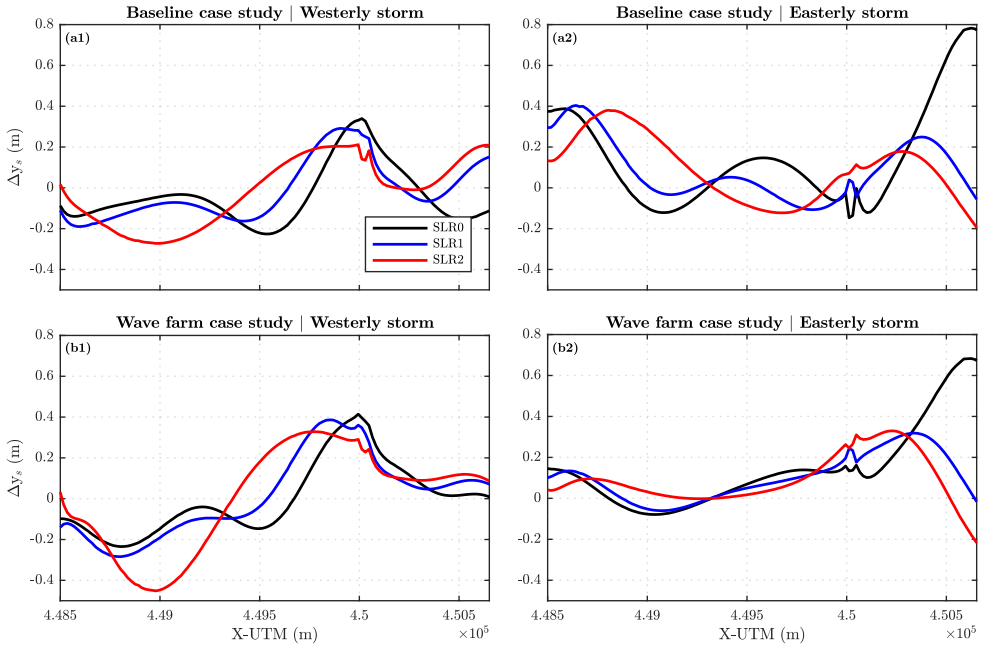


Figure 7: Shoreline advance (Δy_s) after 48 hours without (a) and with (b) wave farm for the westerly (1) and easterly (2) storms. Positive (negative) values mean accretion (erosion).

rise decreases erosion in the central part, turning it to accretion, especially in scenario SLR2. However, accretion in the easternmost part of the beach is decreased in the sea level rise scenarios. For both directions, the results around X-UTM = 450000 m are influenced by the changes in LST patterns and conditioned by the derivative in Eq. 2.

In order to quantify the effect of the wave farm on the variation of the shoreline, the non-dimensional shoreline advance [53] was computed. This indicator can be expressed as:

$$\upsilon = \frac{\Delta y_s - \Delta y_{s0}}{\max\left(|\Delta y_{s0}|\right)}, \tag{3}$$

with Δy_s and Δy_{s0} the variation in the shoreline position with and without wave farm. Positive and negative values indicate accretion or erosion, i.e., advance or retreat of the shoreline, respectively.

The wave farm produces erosion in a narrow zone in the western part of the beach, and accretion in the central and eastern parts of Playa Granada

under the westerly storm (Fig. 8a). It is clear on the graph that sea level rise enhances the impact of the wave farm. In the case of the erosion, the minimum non-dimensional shoreline advance in scenario SLR0 is equal to –0.46, whereas in scenarios SLR1 and SLR2 this value is –0.54 and –0.57, respectively – in other words, erosion (shoreline retreat) is more pronounced. A similar effect may be observed for the accretion (shoreline advance), with maximum values increasing from 0.51 in scenario SLR0 to 0.56 and 0.61 in scenarios SLR1 and SLR2, respectively. Taking into account the whole stretch of coast, accretion due to the presence of the wave farm dominates, with alongshore-averaged values of υ equal to 0.11, 0.10 and 0.09 for scenarios SLR0, SLR1 and SLR2, respectively.

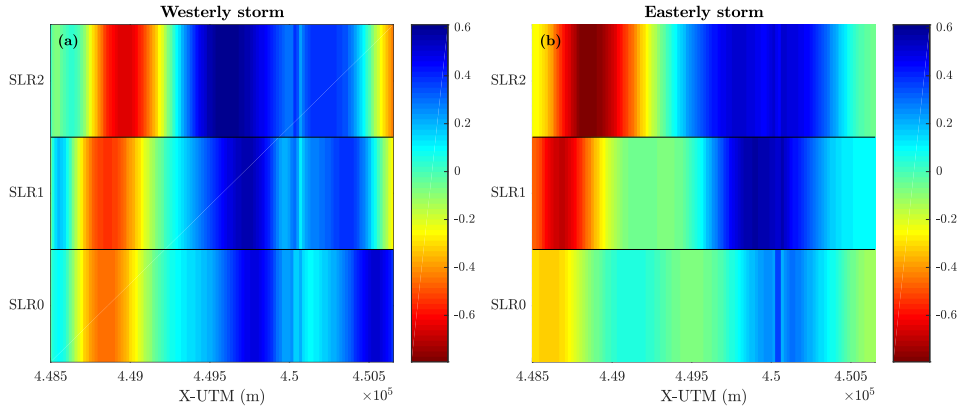


Figure 8: Non-dimensional shoreline advance (υ) for the W (a) and E (b) storms. Positive (negative) values signify accretion (erosion).

Under the easterly storm, a similar impact is produced by the presence of the wave farm, with erosion again in the western part and accretion growing to the east (Fig. 8b). The effect of sea level rise, strengthening the impact – whether positive or negative – of the wave farm, is confirmed. Attending to the erosion in the western end, the minimum value of υ in scenario SLR0 is –0.33, decreasing to –0.69 and –0.79 in scenarios SLR1 and SLR2, respectively. Like erosion, accretion is enhanced by the wave farm, with maximum values ranging from 0.35 in scenario SLR0 to 0.57 and 0.52 in scenarios SLR1 and SLR2,

respectively. The alongshore-averaged values of v under the easterly storm are lower: 0.001, 0.035 and 0.003 for scenarios SLR0, SLR1 and SLR2, respectively.

4.4. Subaerial beach area variation

The final subaerial beach area obtained for the different sea level rise scenarios and the impact produced by the wave farm are presented in this section. Under the westerly storm, the wave farm produces a positive impact in terms of dry beach area. Erosion dominates without the wave farm in the three sea level rise scenarios, with subaerial beach area variations after 48 hours of: –90.15 m^2, –42.83 m^2 and –51.66 m^2 for scenarios SLR0, SLR1 and SLR2, respectively (Fig. 9a). With the presence of the wave farm, this erosion turns into accretion: $\Delta A = 2.31$ m^2, $\Delta A = 28.76$ m^2 and $\Delta A = 8.14$ m^2 in scenarios SLR0, SLR1 and SLR2, respectively. As may be observed in these results, sea level rise decreases erosion without the wave farm, with lower beach area differences, and strengthens the accretionary effect of the wave farm, thus increasing the final subaerial beach area.

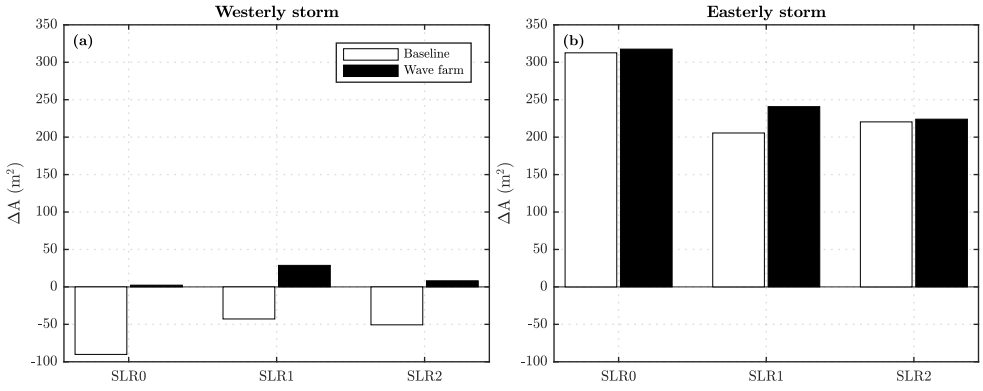


Figure 9: Subaerial beach area variation (ΔA) after 48 hours without (baseline) and with wave farm for the W (a) and E (b) storms.

The behaviour of the system is accretionary under the easterly storm (Fig. 9b), as shown by the subaerial beach area difference in scenario SLR0 without wave farm (312.6 m^2). The results depict that this accretion will be attenuated

by sea level rise, decreasing the area differences to 205.55 m^2 and 220.38 m^2 in scenarios SLR1 and SLR2, respectively. The wave farm would help to mitigate these effects, increasing accretion in every scenario: 317.56 m^2 (SLR0), 240.74 m^2 (SLR1) and 224 m^2 (SLR2).

However, the effect of sea level rise on the beach cannot be fully understood attending only to its impact on the LST and neglecting the loss of subaerial beach area due to the coastal flooding resulting directly from the sea level rise. Figure 10 depicts the total area of Playa Granada in every scenario studied. The subaerial area available in the present situation is 101771 m^2. This area is reduced to 88540 m^2 and 82679 m^2 in scenarios SLR1 and SLR2, respectively. This means that 13231 m^2 will be lost by 2010 according to the optimistic projection, whereas this loss would rise to 19092 m^2 for the pessimistic projection.

The final subaerial beach area after the westerly storm for scenario SLR0 decreases to 101685 m^2, whereas the wave farm increases this area slightly to 101775 m^2. Under the easterly storm, the final area for this scenario with (without) wave farm is 102073 m^2 (102061 m^2). In scenario SLR1, the final area with (without) wave farm under the westerly storm is 88570 m^2 (88497 m^2) under the westerly storm and 88779 m^2 (88741 m^2) under the easterly one. Finally, the final area for the pessimistic projection (scenario SLR2) with (without) wave farm is 82685 m^2 (82624 m^2) under the westerly storm and 82906 m^2 (82900 m^2) under the easterly storm.

These results show that due to sea level rise, between 13% and 19% of the subaerial beach surface will be lost by 2100. In all the scenarios considered, the effect of the wave farm is to increase the final subaerial beach area.

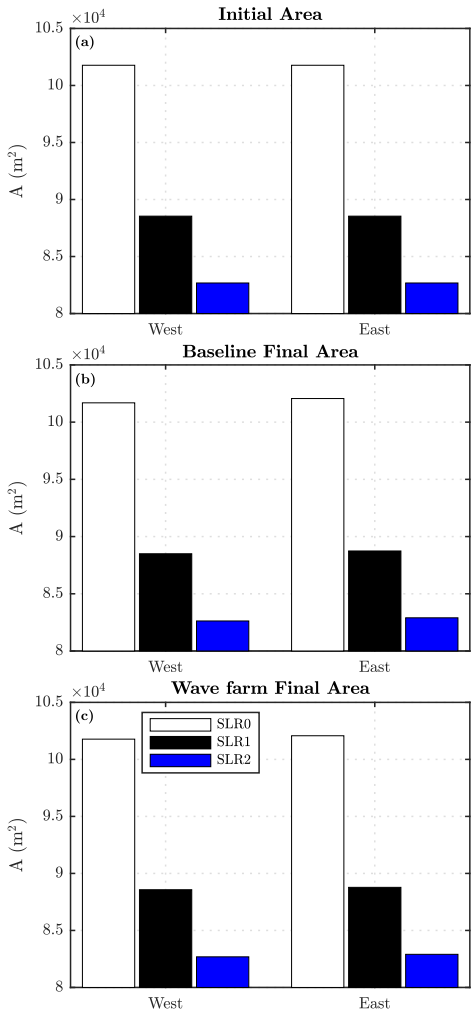


Figure 10: Initial and final subaerial beach area for the three sea level rise scenarios without and with wave farm.

5. Discussion

A number of research works have dealt with the coastal protection performance provided by wave farms. For sandy beaches, [50–52] studied the effects of wave farms on the beach profile in a storm scale. In the case of gravel dominated beaches, recent works have studied the influence of different parameters and conditions such as the alongshore position [54] or the wave farm layout [53, 57]. However, none of these works have studied the repercussions of sea level rise on the coastal protection againts erosion provided by a wave farm, which is the main motivation of this study.

The significance of this work lies in the fact that the results highlight the efficiency of wave farms in coastal protection even in a sea level rise context. In this manner, dual wave farms – for carbon-free energy generation and coastal defence against erosion – become more attractive, since they can contribute to two of the major challenges of the 21st century: the decarbonisation of the energy mix and the mitigation of the impacts of climate change. This fact enhances their interest as coastal defence elements against traditional hard-engineering solutions, such as groynes or seawalls, which are not able to maintain the same efficiency under a sea level rise conditions.

However, further research is required in this field. To fully take into account the effects of sea level rise, research efforts focused on addressing the sea level rise implications in coastal protection in the long-term scale are required.

6. Conclusions

Climate change has repercussions for the world's coastlines, notably through sea level rise and consequent erosion. Recent works have proposed the use of wave farms with a dual purpose: carbon-free energy generation and coastal protection. This work investigated the effects of a so-called dual wave farm on a gravel-dominated beach and, for the first time, considered how these effects were themselves modified by sea level rise. Using a spectral wave propagation model (SWAN), a LST formulation and a one-line model, the final position of

the shoreline and final subaerial beach areas were calculated for three sea level rise scenarios: present situation (SLR0), and optimistic (SLR1) and pessimistic (SLR2) projections.

The presence of the wave farm reduces the significant wave height at breaking, with alongshore-averaged ratios with respect to the no-wave farm situation of 0.79 - 0.80 (0.97 - 0.98) for the easterly (westerly) storm. Sea level rise enhances the coastal protection efficiency of the wave farm by reducing the minimum ratios.

The reduction in significant wave height at breaking caused by the wave farm leads to a reduction in LST rates, with alongshore-averaged ratios with respect to the no-wave farm situation of 0.92 - 0.95 (0.51 - 0.52) for the westerly (easterly) storm. Sea level rise contributes to this positive effect of the wave farm, reducing the ratios of alongshore-averaged LST rates, especially for the westerly storm.

The shoreline shows accretion in the eastern part of the beach due to the presence of the wave farm, for both the westerly and easterly storms. However, some erosion appears in the western end. If the final (post-storm) subaerial beach area is considered, the effect of the wave farm is positive, i.e., accretionary. In the case of the westerly storm, the wave farm reverses the behaviour of the coast from an erosive to an accretionary response in every sea level rise scenario. Without the wave farm the subaerial beach area differences are –90.15 m^2, –42.83 m^2 and –51.66 m^2 for scenarios SLR0, SLR1 and SLR2, respectively; with the wave farm these differences are 2.31 m^2, 28.76 m^2 and 8.14 m^2. Under the easterly storm, the coastal response is accretionary, and this behaviour is strengthened by the wave farm.

Acknowledgements

This paper was supported by the research grants WAVEIMPACT (PCIG-13-GA-2013-618556, European Commission, Marie Curie fellowship, fellow GI) and ICE (Intelligent Community Energy, European Commision, Contract no.

5025). RB was partly funded by the Spanish Ministry of Science, Innovation and Universities (*Programa Juan de la Cierva 2017*, FJCI-2017-31781). Wave and bathymetric data were provided by *Puertos del Estado* (Spain) and the Spanish Ministry of Agriculture, Fisheries and Food, respectively. We thank two anonymous reviewers for their improvements to this work.

References

[1] B. Atilgan, A. Azapagic, Life cycle environmental impacts of electricity from fossil fuels in Turkey, Journal of Cleaner Production 106 (2015) 555–564.

[2] Y. Achawangkul, N. Maruyama, M. Hirota, C. Chaichana, S. Sedpho, T. Sutabutr, Evaluation on environmental impact from the utilization of fossil fuel, electricity and biomass producer gas in the double-chambered crematories, Journal of Cleaner Production 134 (2016) 463–468.

[3] P. K. Wesseh Jr, B. Lin, Options for mitigating the adverse effects of fossil fuel subsidies removal in Ghana, Journal of Cleaner Production 141 (2017) 1445–1453.

[4] F. Dalir, M. S. Motlagh, K. Ashrafi, A dynamic quasi comprehensive model for determining the carbon footprint of fossil fuel electricity: A case study of Iran, Journal of Cleaner Production 188 (2018) 362–370.

[5] Intergovernmental Panel on Climate Change, Climate change 2014: synthesis report, IPCC Geneva, Switzerland, 2014.

[6] L. M. Abadie, Sea level damage risk with probabilistic weighting of IPCC scenarios: An application to major coastal cities, Journal of Cleaner Production 175 (2018) 582–598.

[7] European Commission, A European Strategic Energy Technology Plan (Set-Plan): Towards a low carbon future, Brussels: Commission of the European Communities (2007).

[8] J. Huenteler, C. Niebuhr, T. S. Schmidt, The effect of local and global learning on the cost of renewable energy in developing countries, Journal of Cleaner Production 128 (2016) 6 – 21.

[9] P. Nie, Y. Chen, Y. Yang, X. Henry Wang, Subsidies in carbon finance for promoting renewable energy development, Journal of Cleaner Production 139 (2016) 677 – 684.

[10] M. O. A. González, J. S. Gonalves, R. M. Vasconcelos, Sustainable development: Case study in the implementation of renewable energy in Brazil, Journal of Cleaner Production 142 (2017) 461 – 475.

[11] C. Kung, L. Zhang, M. Chang, Promotion policies for renewable energy and their effects in taiwan, Journal of Cleaner Production 142 (2017) 965 – 975.

[12] R. Maqbool, Y. Sudong, Critical success factors for renewable energy projects; empirical evidence from Pakistan, Journal of Cleaner Production (2018).

[13] H. L. Mendonça, M. V. d. A. Fonseca, et al., Working towards a framework based on mission-oriented practices for assessing renewable energy innovation policies, Journal of Cleaner Production 193 (2018) 709–719.

[14] F. J. Ramírez, A. Honrubia-Escribano, E. Gómez-Lázaro, D. T. Pham, The role of wind energy production in addressing the European renewable energy targets: The case of Spain, Journal of Cleaner Production (2018).

[15] X. Ruhang, S. Zixin, T. Qingfeng, Y. Zhuangzhuang, The cost and marketability of renewable energy after power market reform in China: A review, Journal of Cleaner Production 204 (2018) 409–424.

[16] T. N. Sequeira, M. S. Santos, Renewable energy and politics: A systematic review and new evidence, Journal of Cleaner Production 192 (2018) 553–568.

[17] A. Sinha, M. Shahbaz, T. Sengupta, Renewable Energy Policies and Contradictions in Causality: A case of Next 11 Countries, Journal of Cleaner Production 197 (2018) 73–84.

[18] R. Waheed, D. Chang, S. Sarwar, W. Chen, Forest, agriculture, renewable energy, and CO2 emission, Journal of Cleaner Production 172 (2018) 4231–4238.

[19] X.-C. Yuan, Y.-J. Lyu, B. Wang, Q.-H. Liu, Q. Wu, China's energy transition strategy at the city level: The role of renewable energy, Journal of Cleaner Production 205 (2018) 980–986.

[20] A. Clément, P. McCullen, A. F. de O. Falcão, A. Fiorentino, F. Gardner, K. Hammarlund, G. Lemonis, T. Lewis, K. Nielsen, S. Petroncini, M.-T. Pontes, P. Schild, B.-O. Sjöström, H. C. Sørensen, T. Thorpe, Wave energy in Europe: current status and perspectives, Renewable and Sustainable Energy Reviews 6 (2002) 405–431.

[21] A. M. Cornett, A global wave energy resource assessment, in: The Eighteenth International Offshore and Polar Engineering Conference, International Society of Offshore and Polar Engineers, 2008.

[22] J. Cruz, Ocean wave energy: current status and future prespectives, Springer Science & Business Media, 2008.

[23] A. F. de O. Falcão, Modelling and control of oscillating-body wave energy converters with hydraulic power take-off and gas accumulator, Ocean Engineering 34 (2007) 2021–2032.

[24] P. Contestabile, C. Iuppa, E. D. Lauro, L. Cavallaro, T. L. Andersen, D. Vicinanza, Wave loadings acting on innovative rubble mound breakwater for overtopping wave energy conversion, Coastal Engineering 122 (2017) 60 – 74.

[25] H. Fernandez, G. Iglesias, R. Carballo, A. Castro, J. Fraguela, F. Taveira-Pinto, M. Sanchez, The new wave energy converter WaveCat: Concept and laboratory tests, Marine Structures 29 (2012) 58–70.

[26] I. López, B. Pereiras, F. Castro, G. Iglesias, Optimisation of turbine-induced damping for an OWC wave energy converter using a RANS–VOF numerical model, Applied Energy 127 (2014) 105 – 114.

[27] E. Medina-López, R. Bergillos, A. Moñino, M. Clavero, M. Ortega-Sánchez, Effects of seabed morphology on oscillating water column wave energy converters, Energy 135 (2017) 659–673.

[28] A. Moñino, E. Medina-López, R. J. Bergillos, M. Clavero, A. Borthwick, M. Ortega-Sánchez, Thermodynamics and Morphodynamics in Wave Energy, Springer, 2018.

[29] E. Medina-López, A. Moñino, R. Bergillos, M. Clavero, M. Ortega-Sánchez, Oscillating water column performance under the influence of storm development, Energy 166 (2019) 765–774.

[30] G. Iglesias, R. Carballo, Choosing the site for the first wave farm in a region: A case study in the Galician Southwest (Spain), Energy 36 (2011) 5525–5531.

[31] R. Carballo, M. Sánchez, V. Ramos, J. Fraguela, G. Iglesias, The intra-annual variability in the performance of wave energy converters: A comparative study in N Galicia (Spain), Energy 82 (2015) 138 – 146.

[32] M. López, M. Veigas, G. Iglesias, On the wave energy resource of Peru, Energy Conversion and Management 90 (2015) 34 – 40.

[33] D. Silva, A. R. Bento, P. Martinho, C. G. Soares, High resolution local wave energy modelling in the Iberian Peninsula, Energy 91 (2015) 1099–1112.

[34] A. Viviano, S. Naty, E. Foti, T. Bruce, W. Allsop, D. Vicinanza, Large-scale experiments on the behaviour of a generalised oscillating water column under random waves, Renewable Energy 99 (2016) 875 – 887.

[35] A. López-Ruiz, R. J. Bergillos, M. Ortega-Sánchez, The importance of wave climate forecasting on the decision-making process for nearshore wave energy exploitation, Applied Energy 182 (2016) 191–203.

[36] A. López-Ruiz, R. J. Bergillos, A. Lira-Loarca, M. Ortega-Sánchez, A methodology for the long-term simulation and uncertainty analysis of the operational lifetime performance of wave energy converter arrays, Energy 153 (2018) 126–135.

[37] A. López-Ruiz, R. J. Bergillos, J. M. Raffo-Caballero, M. Ortega-Sánchez, Towards an optimum design of wave energy converter arrays through an integrated approach of life cycle performance and operational capacity, Applied Energy 209 (2018) 20–32.

[38] C. Pérez-Collazo, D. Greaves, G. Iglesias, A review of combined wave and offshore wind energy, Renewable and Sustainable Energy Reviews 42 (2015) 141 – 153.

[39] S. Astariz, C. Perez-Collazo, J. Abanades, G. Iglesias, Towards the optimal design of a co-located wind-wave farm, Energy 84 (2015) 15 – 24.

[40] S. Astariz, J. Abanades, C. Perez-Collazo, G. Iglesias, Improving wind farm accessibility for operation and maintenance through a co-located wave farm: Influence of layout and wave climate, Energy Conversion and Management 95 (2015) 229 – 241.

[41] P. Contestabile, E. Di Lauro, M. Buccino, D. Vicinanza, Economic Assessment of Overtopping BReakwater for Energy Conversion (OBREC): A Case Study in Western Australia, Sustainability 9 (2016).

[42] S. Astariz, G. Iglesias, The economics of wave energy: A review, Renewable and Sustainable Energy Reviews 45 (2015) 397 – 408.

[43] S. Astariz, A. Vazquez, G. Iglesias, Evaluation and comparison of the levelized cost of tidal, wave, and offshore wind energy, Journal of Renewable and Sustainable Energy 7 (2015) 053112.

[44] S. Astariz, G. Iglesias, Wave energy vs. other energy sources: A reassessment of the economics, International Journal of Green Energy 13 (2016) 747–755.

[45] M. I. Vousdoukas, L. Mentaschi, E. Voukouvalas, A. Bianchi, F. Dottori, L. Feyen, Climatic and socioeconomic controls of future coastal flood risk in Europe, Nature Climate Change 8 (2018) 776–780.

[46] M. I. Vousdoukas, L. Mentaschi, E. Voukouvalas, M. Verlaan, S. Jevrejeva, L. P. Jackson, L. Feyen, Global probabilistic projections of extreme sea levels show intensification of coastal flood hazard, Nature Communications 9 (2018) 2360.

[47] J. M. Sayol, M. Marcos, Assessing Flood Risk Under Sea Level Rise and Extreme Sea Levels Scenarios: Application to the Ebro Delta (Spain), Journal of Geophysical Research: Oceans 123 (2018) 794–811.

[48] E. J. Anthony, N. Marriner, C. Morhange, Human influence and the changing geomorphology of Mediterranean deltas and coasts over the last 6000 years: From progradation to destruction phase?, Earth-Science Reviews 139 (2014) 336–361.

[49] J. P. M. Syvitski, A. J. Kettner, I. Overeem, E. W. H. Hutton, M. T. Hannon, G. R. Brakenridge, J. Day, C. Vörösmarty, Y. Saito, L. Giosan, R. J. Nicholls, Sinking deltas due to human activities, Nature Geoscience 2 (2009) 681–686.

[50] J. Abanades, D. Greaves, G. Iglesias, Coastal defence through wave farms, Coastal Engineering 91 (2014) 299–307.

[51] J. Abanades, D. Greaves, G. Iglesias, Wave farm impact on the beach profile: A case study, Coastal Engineering 86 (2014) 36–44.

[52] J. Abanades, D. Greaves, G. Iglesias, Wave farm impact on beach modal state, Marine Geology 361 (2015) 126–135.

[53] C. Rodriguez-Delgado, R. J. Bergillos, M. Ortega-Sánchez, G. Iglesias, Protection of gravel-dominated coasts through wave farms: Layout and shoreline evolution, Science of The Total Environment 636 (2018) 1541 – 1552.

[54] C. Rodriguez-Delgado, R. J. Bergillos, M. Ortega-Sánchez, G. Iglesias, Wave farm effects on the coast: The alongshore position, Science of The Total Environment 640-641 (2018) 1176 – 1186.

[55] R. J. Bergillos, A. López-Ruiz, E. Medina-López, A. Moñino, M. Ortega-Sánchez, The role of wave energy converter farms on coastal protection in eroding deltas, Guadalfeo, southern Spain, Journal of Cleaner Production 171 (2018) 356 – 367.

[56] R. J. Bergillos, C. Rodriguez-Delgado, G. Iglesias, Wave farm impacts on coastal flooding under sea-level rise: a case study in southern spain, Science of the Total Environment, 653 (2019) 1522–1531.

[57] C. Rodriguez-Delgado, R. J. Bergillos, G. Iglesias, Dual wave farms and coastline dynamics: The role of inter-device spacing, Science of The Total Environment 646 (2019) 1241 – 1252.

[58] J. Abanades, G. Flor-Blanco, G. Flor, G. Iglesias, Dual wave farms for energy production and coastal protection, Ocean & Coastal Management 160 (2018) 18 – 29.

[59] L. C. van Rijn, A simple general expression for longshore transport of sand, gravel and shingle, Coastal Engineering 90 (2014) 23 – 39.

[60] R. Pelnard-Considère, Essai de theorie de l'evolution des formes de rivage en plages de sable et de galets, Les Energies de la Mer: Compte Rendu Des Quatriemes Journees de L'hydraulique, Paris 13, 14 and 15 Juin 1956; Question III, rapport 1, 74-1-10 (1956).

[61] R. J. Bergillos, C. Rodríguez-Delgado, A. López-Ruiz, A. Millares, M. Ortega-Sánchez, M. A. Losada, Recent human-induced

coastal changes in the Guadalfeo river deltaic system (southern Spain), in: Proceedings of the 36th IAHR-International Association for Hydro-Environment Engineering and Research World Congress: http://89.31.100.18/~iahrpapers/87178.pdf, 2015.

[62] R. J. Bergillos, M. Ortega-Sánchez, M. A. Losada, Foreshore evolution of a mixed sand and gravel beach: The case of Playa Granada (Southern Spain), in: Proceedings of the 8th Coastal Sediments, World Scientific, 2015.

[63] R. J. Bergillos, M. Ortega-Sánchez, G. Masselink, M. A. Losada, Morpho-sedimentary dynamics of a micro-tidal mixed sand and gravel beach, Playa Granada, southern Spain, Marine Geology 379 (2016) 28–38.

[64] R. J. Bergillos, G. Masselink, R. T. McCall, M. Ortega-Sánchez, Modelling overwash vulnerability along mixed sand-gravel coasts with XBeach-G: Case study of Playa Granada, southern Spain, in: Coastal Engineering Proceedings, volume 1 (35), 2016, p. 13.

[65] R. J. Bergillos, C. Rodríguez-Delgado, A. Millares, M. Ortega-Sánchez, M. A. Losada, Impact of river regulation on a mediterranean delta: Assessment of managed versus unmanaged scenarios, Water Resources Research 52 (2016) 5132–5148.

[66] R. J. Bergillos, M. Ortega-Sánchez, Assessing and mitigating the landscape effects of river damming on the Guadalfeo River delta, southern Spain, Landscape and Urban Planning 165 (2017) 117–129.

[67] R. J. Bergillos, C. Rodríguez-Delgado, M. Ortega-Sánchez, Advances in management tools for modeling artificial nourishments in mixed beaches, Journal of Marine Systems 172 (2017) 1–13.

[68] R. J. Bergillos, A. López-Ruiz, D. Principal-Gómez, M. Ortega-Sánchez, An integrated methodology to forecast the efficiency of nourishment strategies in eroding deltas, Science of the Total Environment 613 (2018) 1175–1184.

[69] M. Ortega-Sánchez, R. J. Bergillos, A. López-Ruiz, M. A. Losada, Morphodynamics of Mediterranean Mixed Sand and Gravel Coasts, Springer, 2017.

[70] R. J. Bergillos, G. Masselink, M. Ortega-Sánchez, Coupling cross-shore and longshore sediment transport to model storm response along a mixed sand-gravel coast under varying wave directions., Coastal Engineering, 129 (2017) 93–104.

[71] R. J. Bergillos, A. López-Ruiz, M. Ortega-Sánchez, G. Masselink, M. A. Losada, Implications of delta retreat on wave propagation and longshore sediment transport-Guadalfeo case study (southern Spain), Marine Geology 382 (2016) 1–16.

[72] G. Iglesias, R. Carballo, A. Castro, B. Fraga, Development and design of the WaveCat^{TM} energy converter, in: Coastal Engineering 2008: (In 5 Volumes), World Scientific, 2009, pp. 3970–3982.

[73] G. Iglesias, H. Fernándes, R. Carballo, A. Castro, F. Taveira-Pinto, The wavecat©-development of a new wave energy converter, in: World Renewable Energy Congress-Sweden; 8-13 May; 2011; Linköping; Sweden, 57, Linköping University Electronic Press, 2011, pp. 2151–2158.

[74] G. Iglesias, R. Carballo, A. Castro, B. Fraga, Development and design of the WaveCat^{TM} energy converter, in: Coastal Engineering 2008: (In 5 Volumes), World Scientific, 2009, pp. 3970–3982.

[75] R. Carballo, G. Iglesias, Wave farm impact based on realistic wave-WEC interaction, Energy 51 (2013) 216–229.

[76] H. Fernandez, G. Iglesias, R. Carballo, A. Castro, M. Sánchez, F. Taveira-Pinto, Optimization of the wavecat wave energy converter, Coastal Engineering Proceedings 1 (2012) 5.

[77] L. Holthuijsen, N. Booij, R. Ris, A spectral wave model for the coastal zone, ASCE, 1993.

[78] E. Rusu, C. G. Soares, Coastal impact induced by a Pelamis wave farm operating in the Portuguese nearshore, Renewable Energy 58 (2013) 34–49.

[79] A. Kieftenburg, A short overview of reflection formulations and suggestions for implementation in SWAN, Technical Report, TU Delft, Department of Hydraulic Engineering, 2001.